High-Spatial-Resolution High-Temperature Sensor Based on Ultra-Short Fiber Bragg Gratings With Dual-Wavelength Differential Detection

Kuikui Guo, Jun He, He Li, Baijie Xu, Shengzhen Lu, Shen Liu, Xizhen Xu, Gaixia Xu, and Yiping Wang, *Senior Member, IEEE*

***Abstract*—Type II fiber Bragg gratings (FBGs) inscribed with femtosecond (*fs*) laser possess significant potential for high temperature sensing. In this work, we propose and demonstrate a method for fabricating a parallel-integrated ultra-short type II FBG (PI-US-FBG) by using an *fs* laser point-by-point technology. The PI-US-FBG, featuring by an ultra-short grating length of 80 μm, consists of six identical FBGs parallel-inscribed into a fiber core at different radial positions in the same cross section. The fabricated PI-US-FBG exhibits a broadband Gaussian-shape spectrum with a low reflectivity of ∼10%, an ultra-low out-of-band insertion loss of 0.01 dB, and a large full width at half maximum bandwidth of 9.4 nm. Moreover, this PI-US-FBG could be used as a high temperature sensor with a wide measurement range from 25 to 1000 °C, and an excellent linearity was achieved with a dual-wavelength differential detection. The temperature sensitivity could be increased from 0.00316 to 0.00945 (dB/ °C) by enlarging the wavelength spacing of the tunable laser. In addition, two cascaded PI-US-FBGs were used to precisely measure the temperature field distribution in a CO_2 laser spot with a very high spatial resolution of 100 μm. Hence, the proposed PI-US-FBGs could be used for a large-scale fiber sensor network, especially in future distributed temperature measurement with a high spatial resolution.**

***Index Terms*—Fiber bragg gratings, fiber optics sensors, laser materials processing.**

Manuscript received October 14, 2021; revised November 20, 2021; accepted November 26, 2021. Date of publication November 30, 2021; date of current version April 4, 2022. This work was supported in part by the National Natural Science Foundation of China (NSFC) under Grants U1913212, 61875128, and 62005170, in part by the Department of Science and Technology of Guangdong Province under Grants 2019TQ05X113, 2019A1515011393, and 2019A1515111114, and in part by Shenzhen Science and Technology Program under Grants RCYX20200714114538160, JCYJ20180507182058432, JCYJ 20200109 114201731, and JCYJ20210324100008024. *(Corresponding author: Jun He.)*

Kuikui Guo, Jun He, He Li, Baijie Xu, Shengzhen Lu, Shen Liu, Xizhen Xu, and Yiping Wang are with the Guangdong and Hong Kong Joint Research Centre for Optical Fibre Sensors, College of Physics and Optoelectronic Engineering, Shenzhen University, Shenzhen 518060, China and also with the Shenzhen Key Laboratory of Photonic Devices and Sensing Systems for Internet of Things, Guangdong and Hong Kong Joint Research Centre for Optical Fibre Sensors, Shenzhen University, Shenzhen 518060, China (e-mail: 2150190116@email.szu.edu.cn; hejun07@szu.edu.cn; 2070456093@email.szu.edu.cn; 1900453046@email.szu.edu.cn; lushengzhen 2019@email.szu.edu.cn; shenliu@szu.edu.cn; xizhenxu@szu.edu.cn; ypwang@szu.edu.cn).

Gaixia Xu is with the Guangdong Key Laboratory for Biomedical Measurements and Ultrasound Imaging, School of Biomedical Engineering, Shenzhen University Health Science Center, Shenzhen 518060, China (e-mail: xugaixia@szu.edu.cn).

Color versions of one or more figures in this article are available at https://doi.org/10.1109/JLT.2021.3131499.

Digital Object Identifier 10.1109/JLT.2021.3131499

I. Introduction

FIBER Bragg gratings (FBGs) have been widely used in many fields of optical fiber sensors, fiber-optic communications, and fiber lasers due to the advantages of compact size, electromagnetic immunity, and multiplexing capability, etc [1]. In general, the FBGs with long grating length always have poor vulnerability to no-uniform physical fields, which could distort the FBG spectrum considerably and badly affect the measurement accuracy [2]. Fortunately, there also exists a type of ultra-short FBGs (US-FBGs) with grating lengths scaled to only hundreds or even tens of microns and can solve the problems mentioned above. Moreover, the US-FBGs could also be used as sensing elements for large-scale distributed sensing networks due to the high spatial resolution [3]. However, the US-FBGs also yield a large bandwidth, which can reach up to several or even tens of nm. This wide reflection spectrum in the US-FBGs is unfavorable for conventional wavelength interrogations. For most commonly used interrogation methods based on tracking the wavelength peak or notch, their broad spectra would prevent a high resolution [2]. To overcome this drawback, Xia *et al.* proposed a new method for interrogating a 450 μm-long US-FBG based on a dual-wavelength differential detection (DWDD) [4]. In 2016, they also reported a large-scale cascaded 500 μm-long US-FBG sensing array based on DWDD [5]. Hence, the DWDD could offer an effective, flexible, and simpler interrogation scheme, opening up exploitation possibility of future US-FBG sensors. However, the US-FBGs induced by UV laser are only suited for operating temperature below 450 °C due to their inadequate thermal stability [1].

Recently, the use of femtosecond (*fs*) lasers have been explored for inscribing type II FBGs in various optical fibers via nonlinear photon absorption and photoionization [6]. These type II gratings with structural changes in fiber core have the potential for high temperature sensing of above 1000 °C [7], [8]. In 2017, Hnatovsky *et al.* reported a 130 μm-long type II US-FBG inscribed with *fs* laser through a phase mask and a slit placed proximately the mask, and the US-FBG exhibited a high thermal stability [9]. Nevertheless, one major drawback of this technology is that the grating pitch is fixed by the phase mask period. Since the *fs* laser point-by-point (PbP) technology was first reported to fabricate an FBG [10], it exhibits great advantages of excellent flexibility, free of hydrogen loading and

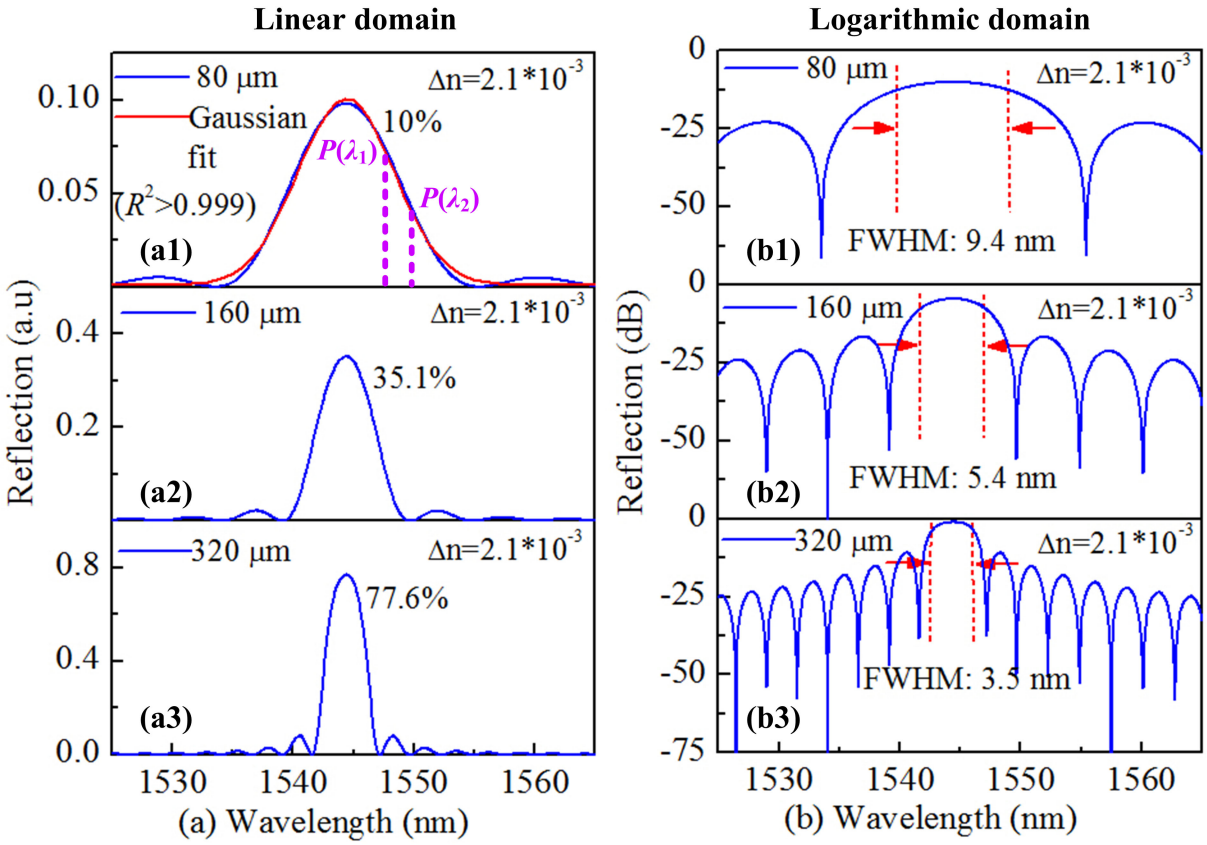

Fig. 1. Simulated reflection spectra of type II FBGs with different grating lengths in case of a fixed refractive index change $\Delta n = 2.1^{*}10^{-3}$ in linear domain (a) and logarithmic domain (b), respectively.

phase mask [11]. Moreover, the refractive index (RI) modified region produced by the *f*s laser PbP method is much smaller than the fiber core diameter, there is only a small overlap between the mode field propagating along the fiber core and the dimension of RI modified region, resulting in a weak coupling coefficient for the US-FBG [12]. The *f*s laser line-by-line (LbL) technology and the *f*s laser plane-by-plane (Pl-b-Pl) technology can increase the coupling coefficient due to the larger RI modified region. However, these two methods (i.e., LbL technology and Pl-b-Pl technology) exhibit no flexibility to adjust the RI modified region [13]. Fortunately, the coupling coefficient can be further enhanced if multiple US-FBGs are parallel inscribed in fiber core via the *f*s laser PbP technology. Meanwhile the RI modified region can be also adjusted by changing the number of the parallel-integrated FBGs (PI-FBGs), and the reflectivity of the grating can be achieved flexible regulation as we expected. Recently, massive efforts have been made to fabricate various PI-FBGs. For example, in 2019, we reported for the first time the fabrication of PI-FBGs with either the same or different resonance wavelengths in fiber core via the *f*s laser PbP method. A 500 μm-long PI-FBG was also fabricated and could realize a spatial resolution of sub-millimeter [14]. Moreover, in 2020, Zhu *et al.* reported the PI-FBGs in fiber core with three distinct resonant wavelengths and used them for a wavelength-switchable fiber laser [15].

In this letter, we demonstrate an 80 μm-long PI-US-FBG with a full width at half maximum (FWHM) bandwidth of 9.4 nm, a low reflectivity of ~10% and an ultra-low insertion loss of 0.01 dB. The fabricated PI-US-FBG consists of six identical gratings which were parallel- inscribed into the fiber core by using the *f*s laser PbP method, and it could be used as a high temperature sensor which could provide a large temperature measurement range by using DWDD scheme. Moreover, a wide tuning range (i.e., 0.00316 to 0.00945 (dB/ °C)) was demonstrated in the temperature sensitivity. In addition, two cascaded PI-US-FBGs were used for measuring the temperature field distribution in the CO_2 laser spot with a high spatial resolution of 100 μm.

II. Principle of Operation

According to the coupled mode theory [16], the spectral profile of a low reflectivity FBG can be modeled as a Gaussian function: $R(\lambda) \propto \exp(-4\ln 2[(\lambda-\lambda_B)/\Delta\lambda_B]^2)$, where λ_B, $\Delta\lambda_B$ are Bragg wavelength and FWHM bandwidth of the grating, respectively. Fig. 1(a) illustrates the calculated reflection spectra of type II FBGs with different grating lengths in case of a fixed RI change $\Delta n = 2.1^{*}10^{-3}$ in linear domain. It is clear that the maximum reflectivity becomes stronger from 10% to 77.6% with the grating length L increases from 80 to 160 μm, as shown

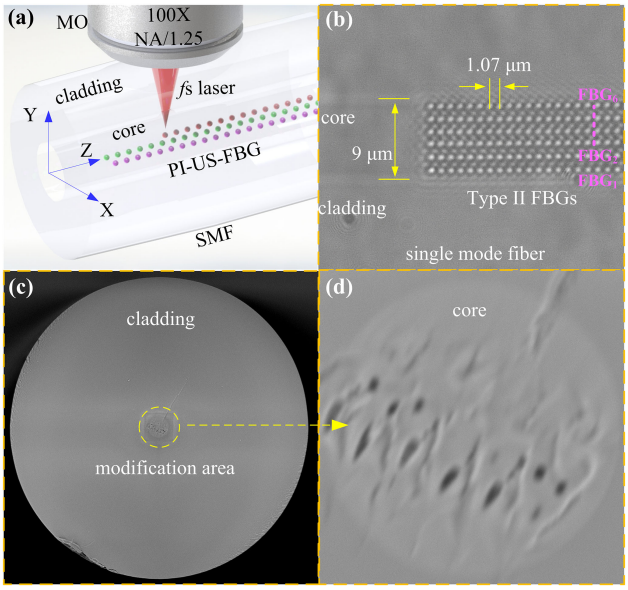

Fig. 2. (a) Schematic of the fabrication of PI-US-FBG by using the *f*s laser PbP technology. (b) Side-view microscope image of the PI-US-FBG. (c) Cross-sectional-view SEM image of the PI-US-FBG. (d) Enlarged view of the RI modified areas in (c).

in Figs. (a1)-(a3), and the reflection spectrum of type II FBG with a low reflectivity of 10% becomes obviously closer to Gaussion profile. A Gaussian fit with an extremely high quality of fit (R^2>0.999) is performed over total reflection spectrum, as shown in Fig. (a1). Additionally, the FWHM bandwidth of type II FBGs becomes narrower from 9.4 to 3.5 nm with the grating length L increases in logarithmic domain, as shown in Figs. (b1)-(b3). Hence, it is concluded that a low reflectivity type II US-FBG with broad Gaussian spectrum could be obtained by decreasing the grating length (i.e., 80 μm) with high RI change.

Since the spectral width of the laser is much narrower than that of the US-FBG, by assuming that laser spectrum and US-FBG spectrum are a delta function and an ideal Gaussian function [3], the total reflected power of the laser from the US-FBG can be expressed as:

$$\mathrm{I} \propto \exp\left[-(4\ln 2)\left(\frac{\lambda_\mathrm{L}-\lambda_\mathrm{B}}{\Delta\lambda_\mathrm{B}}\right)^2\right], \tag{1}$$

where λ_B, λ_L are Bragg wavelength and laser wavelength. Hence, the reflected optical powers (i.e., P(λ_1) and P(λ_2)) of the US-FBG at any two laser wavelength within the grating spectrum, as shown in Fig. 1(a1), will follow two Gaussian behaviors [4]:

$$\mathrm{P}_{\lambda_1}(\lambda_\mathrm{B}) \propto \exp\left[-(4\ln 2)\left(\frac{\lambda_1-\lambda_\mathrm{B}}{\Delta\lambda_\mathrm{B}}\right)^2\right], \tag{2}$$

$$\mathrm{P}_{\lambda_2}(\lambda_\mathrm{B}) \propto \exp\left[-(4\ln 2)\left(\frac{(\lambda_1+\Delta\lambda)-\lambda_\mathrm{B}}{\Delta\lambda_\mathrm{B}}\right)^2\right] \tag{3}$$

where λ_B is the Bragg wavelength of the grating, λ_1, λ_2 are the laser wavelength, and $\Delta\lambda$ is the wavelength spacing between λ_1 and λ_2. By subtracting P(λ_1) and P(λ_2) in log-domain, the

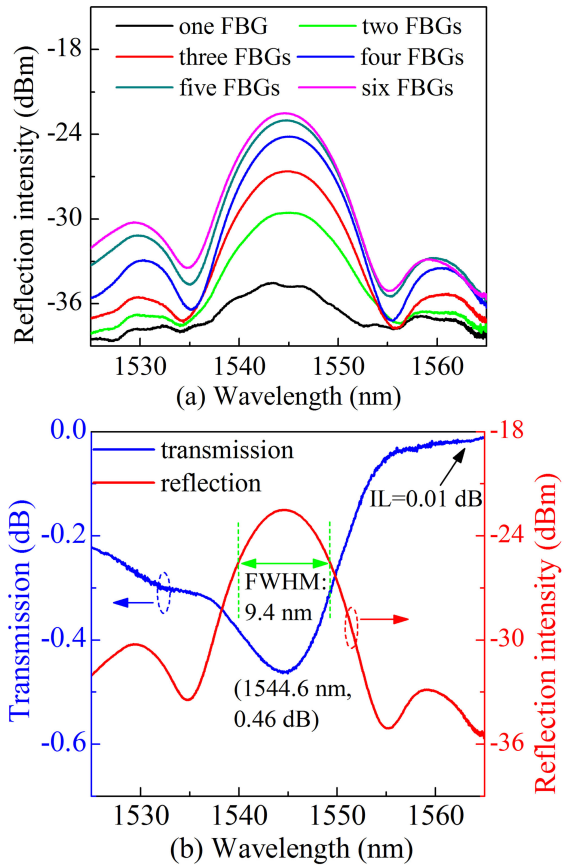

Fig. 3. (a) Reflection spectra evolutions of the fabricated PI-US-FBG with the increase in parallel-integrated gratings. (b) Transmission and reflection spectra of the fabricated PI-US-FBG.

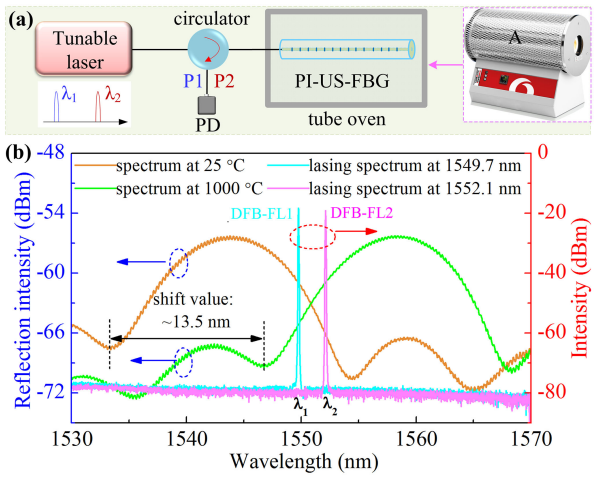

Fig. 4. (a) Experimental setup of high temperature test for the type II PI-US-FBG. (b) Spectra of the tunable laser and the reflected spectra of the type II PI-US-FBG at 25 and 1000 °C.

differential readout of reflected signal can be written as:

$$\mathrm{P}(\lambda_\mathrm{B}) = \lg \mathrm{P}_{\lambda_2}(\lambda_\mathrm{B}) - \lg \mathrm{P}_{\lambda_1}(\lambda_\mathrm{B}) \propto \mathrm{E} + \mathrm{F}^*\lambda_\mathrm{B} \tag{4}$$

where $E = \Delta\lambda^*(\Delta\lambda+2\lambda_1)$ is a constant term for the given case, and $F = -2\Delta\lambda$ is proportional to the wavelength spacing

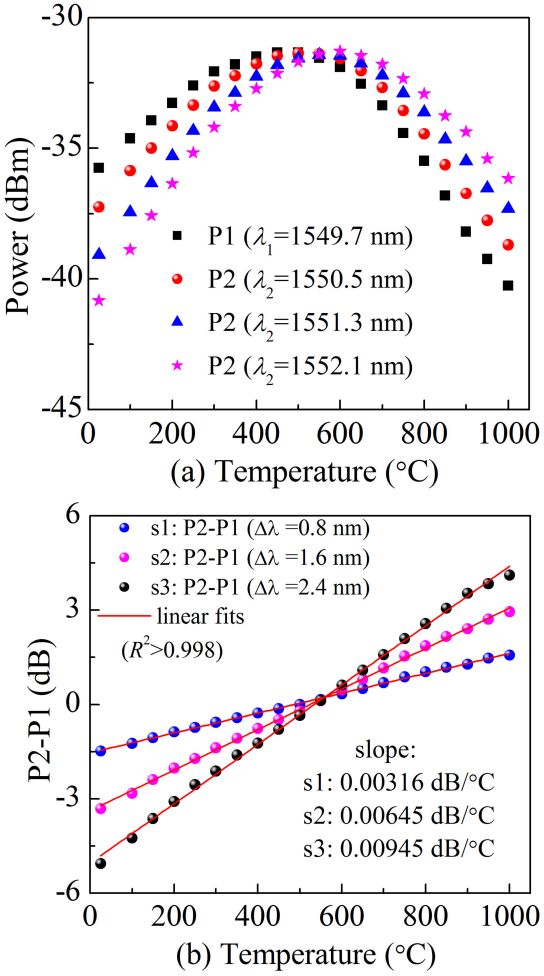

Fig. 5. (a) Reflection intensities (i.e., P1 and P2) versus the temperature. (b) Differential intensity (i.e., P2-P1) as functions of the temperature increase at three different wavelength spacing $\Delta\lambda$.

$\Delta\lambda$. According to Eq. (4), by monitoring intensity difference at any two wavelengths, the Bragg wavelength λ_B shift can be linearly tracked, and the sensitivity F can be tuned by changing wavelength spacing $\Delta\lambda$. Moreover, it is should be noted that the DWDD methods is naturally insensitive to any intensity variations, such as the source fluctuations caused by external vibration.

III. Fabrication of Type II PI-US-FBG

For an FBG inscribed by *f*s laser PbP technology, the coupling coefficient κ can be simplified as $\kappa = \pi\nu\Gamma\Delta n/\lambda$, where ν, Γ are the fringe visibility of RI change Δn and the mode power confinement factor in fiber core [12]. Hence, the coupling coefficient κ could be further enhanced when multiple US-FBGs are parallel-inscribed to increase RI modified areas in fiber core.

Fig. 2(a) demonstrates a schematic diagram of type II PI-US-FBG inscribed by an *f*s laser PbP technology [17]. The grating inscription process employs an *f*s laser amplifier (Light Conversion), with a center wavelength of 513 nm, a pulse duration of 250 fs and a repetition rate of 200 kHz. The *f*s laser beam could be precisely focused into the core of a standard single mode fiber (Corning SMF-28e) using a 100× oil-immersion objective (1.25 NA). The SMF with a core diameter of approximately 9 μm was moved at a constant velocity using three-axis translation stages. Consequently, an FBG could be inscribed into the fiber core along Z axis. Here, the *f*s laser pulse energy is up to 140 nJ to induce high RI change to form type II FBGs due to ultrafast laser-material interactions [8]. Six identical type II US-FBGs, i.e., FBG_n ($n = 1, 2, 3, 4, 5, 6$), with the same grating length and grating pitch were parallel-inscribed at XZ plane, as shown in Fig. 2(b). Fig. 2(c) and (d) show the cross section of the type II PI-US-FBG and the magnified view of the RI modified regions of the fiber core. It is clear that the RI modified regions in fiber core could be significantly increased via this parallel-inscribed method.

During the fabrication process, the reflection spectra of the type II PI-US-FBG were investigated by using a broadband light source with a wavelength range of 1525-1565 nm and an optical spectral analyzer (OSA, Yokagawa AQ6370C) with a resolution of 0.02 nm. As shown in Fig. 2(b), six identical FBGs, i.e., FBG_n ($n = 1, 2, 3, 4, 5, 6$), with the same grating pitch of 1.07 μm and grating length of 80 μm, were parallel-inscribed in the fiber core by the fabrication process described above. The overlap between the mode field propagating along the fiber core and the dimension of RI change could be improved, resulting in higher coupling coefficient, as shown in Fig. 2(d). As shown in Fig. 3(a), it is clear that the Bragg wavelength of the PI-US-FBG remained mostly unchanged. According to Ref. [16], the reflectivity and the FWHM bandwidth of the grating are positive correlation to the coupling coefficient κ. Hence, the reflectivity and the FWHM bandwidth of the PI-US-FBG could be gradually increased with the parallel-integrated grating number increase. Due to the light intensity exhibits an ideal Gaussian distribution in fiber core [18], the reflected light intensity of six identical FBGs at different radial positions is varied. The reflectivity change of PI-US-FBG is quite small when the gratings (i.e., FBG_1 and FBG_6) are inscribed near the boundary between the fiber core and cladding, as shown in Fig. 3(a). Hence, the reflectivity of the total PI-US-FBG is closely related to the grating position. At last, the reflection spectrum of the PI-US-FBG becomes closer to a Gaussian profile with an FWHM bandwidth of 9.4 nm which is well consistent with the simulated result above (seeing Fig. 1(b1)). Moreover, this type II PI-US-FBG exhibits a very low insertion loss (IL) of 0.01 dB, a transmission loss of −0.46 dB, i.e., corresponding to a reflectivity of $\sim$ 10%, as shown in Fig. 3(b). The Bragg wavelength λ_B appears at 1544.6 nm that meets the phase-matching condition given by $m\lambda_B = 2n_{eff}\Lambda$, where m, n_{eff}, Λ are the harmonic order number, the effective RI of fiber core and the grating period [19].

IV. High-Temperature Sensing of Type II PI-US-FBG

Subsequently, the high temperature test was carried out on the fabricated type II PI-US-FBG with DWDD, and the corresponding experimental setup was shown in Fig. 4(a). A tunable laser with a wavelength range of 1450-1650 nm was used as the light source and provided a switchable wavelength between λ_1 and λ_2. This tunable laser exhibits stable output and fast scanning speed

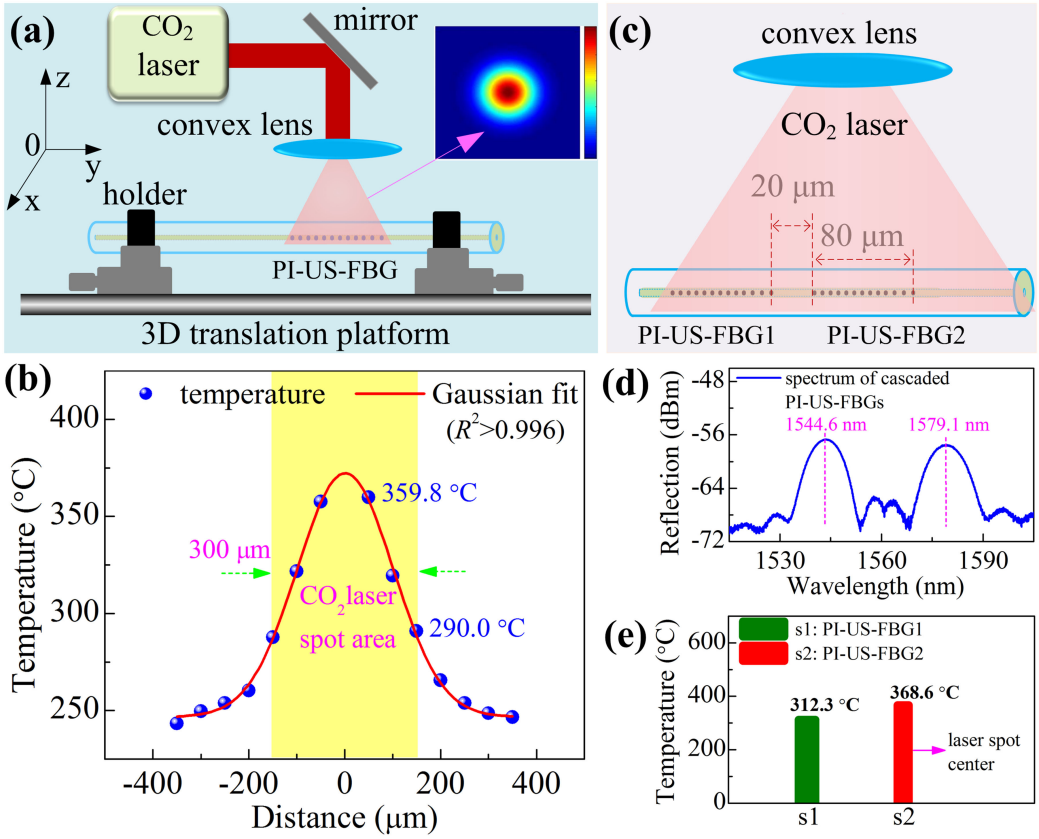

Fig. 6. (a) Experimental setup for measuring temperature distribution in the CO_2 laser spot by using the fabricated PI-US-FBG. (b) Measured temperature distribution of the CO_2 laser spot. (c) Schematic of high-spatial-resolution measurement of the temperature distribution in the CO_2 laser spot by using two cascaded PI-US-FBGs. (d) Reflection spectrum of cascaded PI-US-FBGs. (e) Measured temperature results of cascaded PI-US-FBGs with a high spatial resolution.

(i.e., 200 nm/s), and the reflected optical powers (i.e., P1 and P2) of the grating can be fast obtained. A photodetector (PD) was used for detecting the reflection intensity in log-domain. For an FBG inscribed by the *fs* laser PbP technology, there is a wavelength hysteresis phenomenon during the temperature rise and drop due to the residual stress in fiber core [14]. Hence, this type II PI-US-FBG should be pre-annealed at 500 °C for 48 h to completely relax residual stress.

At first, the reflection spectra of type II PI-US-FBG were recorded at 25 and 1000 °C for 12 hours, as shown in Fig. 4(b). It is clear that the grating spectral shape and reflection intensity almost remain unchanged due to its strong thermal stability, and the Bragg wavelength exhibits a 'red' shift of ~13.5 nm. Hence, the PI-US-FBG exhibits excellent high-temperature stability, and it is very suitable for high temperature sensing. Moreover, the signal-to-noise ratio (SNR) in tunable laser is higher than 60 dB at an output power of −2.0 dBm. The detected lasing wavelengths λ_1 and λ_2 were selected to be at 1549.7 nm and 1552.1 nm, respectively. Note that the lasing wavelengths λ_1, λ_2 should be located at the long wavelength sideband of the grating to allow entire response to characterize the interrogation concept mentioned above.

The high temperature response of the proposed type II PI-US-FBG was investigated in detail via DWDD. Here, the grating was placed in the center of the tube oven, i.e., location A (seeing Fig. 4(a)). At each temperature, the test duration was set to 10 mins to acquire a stable intensity. To prove its adjustable temperature sensitivity, three similar measurements were conducted with different wavelength separations, i.e., by choosing λ_2 to be 1550.5, 1551.3, and 1552.1 nm in each test while keeping constant $\lambda_1 = 1549.7$ nm. Fig. 5(a) plots the recorded reflection powers (i.e., P1 and P2) versus the temperature from 25 to 1000 °C in steps of 100 °C. The recorded intensity responses almost follow a Gaussion behavior as expected due to the Gaussian-shape spectrum of the type II PI-US-FBG. Fig. 5(b) shows the differential intensity (i.e., P2-P1) as functions of the temperature increase at different wavelength spacing, i.e., $\Delta\lambda = 0.8$, 1.6, and 2.4 nm, respectively. A high linearity (i.e., R^2>0.998) between the differential intensity (i.e., P2-P1) and the temperature is observed. Additionally, the temperature sensitivity is proportional to the wavelength spacing, and can be increased from 0.00316 to 0.00945 (dB/ °C) by enlarging the wavelength spacing. The experimental results are consistent with theoretical analysis above (i.e., Eq. (4)).

Furthermore, the temperature distribution in a CO_2 laser spot is measured by using the fabricated PI-US-FBG, which has a grating length (i.e., 80 μm) of less than the laser spot diameter (i.e., ~300 μm). The experimental setup for measuring the temperature field distribution in a CO_2 laser illumination is shown in Fig. 6(a). The CO_2 laser beam with a power of 680 mW was passed through a convex lens and illuminated on the PI-US-FBG. The position of the grating could be precisely adjusted by using

a three-axis translation stage. Generally, the cross-sectional field of CO_2 laser spot exhibits nearly Gaussian distribution (seeing the inset of Fig. 6(a)), which could lead to non-uniform temperature distribution [20]. In the experiment, the intensities (i.e., P1 and P2) at the lasing wavelength λ_1 and λ_2 were recorded when the PI-US-FBG was translated perpendicular to the CO_2 laser with a step of 50 μm. Hence, the temperature at different position could be calculated from Eq. (4) in case of the lasing wavelength $\lambda_1 = 1549.7$ nm and $\lambda_2 = 1552.1$ nm, respectively. Fig. 6(b) shows the temperature distribution of the CO_2 laser spot, and the center temperature and boundary temperature of the CO_2 laser spot are $\sim$ 359.8 °C and $\sim$ 290.0 °C, respectively. It is clear that the temperature at different laser spot locations exhibits a near-Gaussian distribution with a fit of R^2>0.996.

At last, a fiber sensor array consists of two cascaded PI-US-FBGs with a grating length of 80 μm and a spatial spacing of 20 μm was used for a high-spatial-resolution temperature measurement, as shown in Fig. 6(c). Fig. 6(d) shows the measured reflection spectrum of the cascaded two PI-US-FBGs with different Bragg wavelengths at 1544.6 and 1579.1 nm due to the different grating periods, i.e., 1.07 and 1.09 μm, respectively. These two cascaded PI-US-FBGs both exhibit a broadband Gaussian-shape spectrum with a low reflectivity of $\sim$10%, and a large FWHM bandwidth of $\sim$9.4 nm. Here, the wavelength spacing $\Delta\lambda$ is set the same value (i.e., $\Delta\lambda = 2.4$ nm) when the cascaded PI-US-FBGs was used for a high temperature measurement. Hence, the temperature at the PI-US-FBG1 could be calculated from Eq. (4) in case of the lasing wavelength $\lambda_1 = 1549.7$ nm and $\lambda_2 = 1552.1$ nm, and the temperature at the PI-US-FBG2 could be calculated from Eq. (4) in case of the lasing wavelength $\lambda'_1 = 1584.2$ nm and $\lambda'_2 = 1586.6$ nm. Then the CO_2 laser beam with a power of 680 mW was used for illuminating the PI-US-FBG sensor array, and the measured temperature result is shown in Fig. 6(e). The temperatures at PI-US-FBG1 and PI-US-FBG2 are 312.3 °C and 368.6 °C, and the temperature gradient can reach up to 56.3 °C when the PI-US-FBG2 was located in center of the CO_2 laser beam. As a result, these cascaded PI-US-FBGs are very suitable for use as a high temperature sensor with a high spatial resolution of 100 μm.

V. Conclusion

In summary, an 80 μm-long type II PI-US-FBG with an FWHM bandwidth of 9.4 nm was successfully inscribed by using *f*s laser PbP technology. The fabricated PI-US-FBG exhibits a broadband Gaussian-shape spectrum with a low reflectivity of $\sim$10%, an ultra-low out-of-band insertion loss of 0.01 dB. The PI-US-FBG can be used to realize high temperature (>1000 °C) sensing based on a novel DWDD scheme, and a wide temperature sensitivity tuning range of 0.00316 to 0.00945 (dB/ °C) is obtained. Moreover, two cascaded PI-US-FBGs could be used to accurately measure the temperature field distribution with a very high spatial resolution of 100 μm. Hence, the proposed PI-US-FBGs could be used for high-spatial-resolution high-temperature sensing in many industrial applications, such as laser cutting, lasing welding, and device packaging, etc.

References

[1] J. Canning, "Fibre gratings and devices for sensors and lasers," *Laser Photon. Rev.*, vol. 2, no. 4, pp. 275–289, 2008.

[2] R. Cheng, L. Xia, Y. Ran, J. Rohollahnejad, J. Zhou, and Y. Wen, "Interrogation of ultrashort bragg grating sensors using shifted optical gaussian filters," *IEEE Photon. Technol. Lett.*, vol. 27, no. 17, pp. 1833–1836, Sep. 2015.

[3] J. Rohollahnejad *et al.*, "TDM interrogation of intensity-modulated USFBGs network based on multichannel lasers," *Opt. Exp.*, vol. 25, no. 2, pp. 670–680, 2017.

[4] R. Cheng and L. Xia, "Interrogation of weak bragg grating sensors based on dual-wavelength differential detection," *Opt. Lett.*, vol. 41, no. 2, pp. 5254–5257, 2016.

[5] R. Cheng *et al.*, "Ultra-short FBG based distributed sensing using shifted optical gaussian filters and microwave-network analysis," *Opt. Exp.*, vol. 24, no. 3, pp. 2466–2484, 2016.

[6] D. Grobnic, S. J. Mihailov, J. Ballato, and P. D. Dragic, "Type i and II bragg gratings made with infrared femtosecond radiation in high and low alumina content aluminosilicate optical fibers," *Optica*, vol. 2, no. 4, pp. 313–322, 2015.

[7] J. He *et al.*, "Negative-index gratings formed by femtosecond laser overexposure and thermal regeneration," *Sci. Rep.*, vol. 6, no. 10, pp. 1–9, 2016.

[8] S. J. Mihailov, C. Hnatovsky, and D. Grobnic, "Novel type II bragg grating structures in silica fibers using femtosecond lasers and phase masks," *J. Lightw. Technol.*, vol. 37, no. 11, pp. 2549–2556, 2019.

[9] C. Hnatovsky, D. Grobnic, and S. J. Mihailov, "Through-the-coating femtosecond laser inscription of very short fiber bragg gratings for acoustic and high temperature sensing applications," *Opt. Exp.*, vol. 25, no. 21, pp. 25435–25446, 2017.

[10] A. Martinez, M. Dubov, I. Khrushchev, and I. Bennion, "Direct writing of fibre bragg gratings by femtosecond laser," *Electron. Lett.*, vol. 40, no. 19, pp. 1170–1172, 2004.

[11] C. W. Smelser, S. J. Mihailov, and D. Grobnic, "Hydrogen loading for fiber grating writing with a femtosecond laser and a phase mask," *Opt. Lett.*, vol. 29, no. 18, pp. 2127–2129, 2004.

[12] P. Lu *et al.*, "Plane-by-Plane inscription of grating structures in optical fibers," *J. Lightw. Technol.*, vol. 36, no. 4, pp. 926–931, 2018.

[13] P. Roldan-Varona, D. Pallares-Aldeiturriaga, L. Rodriguez-Cobo, and J. M. Lopez-Higuera, "Slit beam shaping technique for femtosecond laser inscription of enhanced Plane-by-Plane FBGs," *J. Lightw. Technol.*, vol. 38, no. 16, pp. 4526–4532, 2020.

[14] Y. Wang *et al.*, "Parallel-integrated fiber Bragg gratings inscribed by femtosecond laser Point-by-Point technology," *J. Lightw. Technol.*, vol. 37, no. 10, pp. 2185–2193, 2019.

[15] W. He, J. Zhao, M. Dong, F. Meng, and L. Zhu, "Wavelength-switchable erbium-doped fiber laser incorporating fiber bragg grating array fabricated by infrared femtosecond laser inscription," *Opt. Laser Technol.*, vol. 127, pp. 1–7, 2020.

[16] T. Erdogan, "Fiber grating spectra," *J. Lightw. Technol.*, vol. 15, no. 8, pp. 1277–1294, 1997.

[17] X. Xu *et al.*, "Sapphire fiber bragg gratings inscribed with a femtosecond laser line-by-line scanning technique," *Opt. Lett.*, vol. 43, no. 19, pp. 4562–4565, 2018.

[18] F. C. Zhang, X. Z. Xu, J. He, B. Du, and Y. P. Wang, "Highly sensitive temperature sensor based on a polymer-infiltrated Mach-Zehnder interferometer created in graded index fiber," *Opt. Lett.*, vol. 44, no. 10, pp. 2466–2469, 2019.

[19] J. Thomas, C. Voigtlaender, R. G. Becker, D. Richter, A. Tuennermann, and S. Nolte, "Femtosecond pulse written fiber gratings: A new avenue to integrated fiber technology," *Laser Photon. Rev*, vol. 6, no. 6, pp. 709–723, 2012.

[20] R. Li, Y. Jin, Z. Li, and K. Qi, "A comparative study of high-power diode laser and CO2 laser surface hardening of AISI 1045 steel," *J. Mater. Eng. Perform.*, vol. 23, no. 9, pp. 3085–3091, 2014.

Kuikui Guo was born in Henan, China, in 1988. He received the B.S. degree from the Institute of Photoelectric Information, Changchun University of Science and Technology, Changchun, China, in 2013, and the Ph.D. degree in optical engineering from Shenzhen University, Shenzhen, China, in 2020. From 2013 to 2015, he was an Optical Engineer with Accu-Tech Co. Ltd, Beijing, China. Since 2020, he has been a Postdoctoral Researcher with the Guangdong and Hong Kong Joint Research Centre for Optical Fiber Sensors, Shenzhen University. His current research interests include optical fiber laser sensors and fiber Bragg gratings.

Jun He was born in Hubei, China, in 1985. He received the B.Eng. degree in electronic science and technology from Wuhan University, Wuhan, China, in 2006, and the Ph.D. degree in electrical engineering from the Institute of Semiconductors, Chinese Academy of Sciences, Beijing, China, in 2011. From 2011 to 2013, he was a Research Engineer with Huawei Technologies, Shenzhen, China. From 2013 to 2015, he was affiliated with Shenzhen University, Shenzhen, China, as a Postdoctoral Research Fellow. From 2015 to 2016, he was a Visiting Fellow with The University of New South Wales, Sydney, NSW, Australia. Since 2017, he has been with Shenzhen University, as an Assistant Professor/Associate Professor. He has authored or coauthored four patent applications and more than 80 journal and conference papers. His current research interests include optical fiber sensors, fiber Bragg gratings (FBGs), and fiber lasers. Dr. He is a Member of the Optical Society of America.

He Li was born in Jilin, in 1998. He received the B.S. degree from the College of Opto-electronic Engineering, Changchun University of Science and Technology, Changchun, China, in 2020. He is currently working toward the M.S. degree with Shenzhen University, Shenzhen, China. His current research interests include femtosecond laser micromachining and sapphire fiber Bragg gratings.

Baijie Xu was born in Guangdong, China, in 1996. He received the B.Eng. degree in 2019 in optoelectronic information science and engineering from Shenzhen University, Shenzhen, China, where he is currently working toward the master's degree in optical engineering. His main research interests include optical fiber sensing and femtosecond laser processing.

Shengzhen Lu was born in 1997. She received the B.S. degree in physics from Lingnan Normal University, Zhanjiang, China, in 2019. She is currently working toward the master's degree in optical engineering with Shenzhen University, Shenzhen, China. Her research focuses on high-Q WGMs resonator.

Shen Liu was born in Henan, China, in 1986. He received the M.S. degree in circuit and system from the Chongqing University of Posts and Telecommunications, Chongqing, China, in 2013, and the Ph.D. degree in optical engineering from Shenzhen University, Shenzhen, China, in 2017. From 2017 to 2018, he was a Postdoctoral Fellow with Aston University, Birmingham, U.K. Since 2018, he has been with Shenzhen University, as an Assistant Professor. He has authored or coauthored 11 patent applications and more than 30 journal and conference papers. His current research interests include optical fiber sensors, WGMs resonator, and cavity optomechanics.

Xizhen Xu was born in Guangdong, China, in 1990. He received the B.S. degree from the College of Science, Zhejiang University of Technology, Hangzhou, China, in 2013, and the Ph.D. degree in optical engineering from Shenzhen University, Shenzhen, China, in 2016 and 2019. From 2019 to 2021, he was a Postdoctoral Research Fellow with Shenzhen University, Shenzhen, China. Since 2021, he has been with Shenzhen University, as an Assistant Professor. He has authored or coauthored three patent applications and more than 20 journal and conference papers. His current research interests include femtosecond laser micromachining, optical fiber sensors, and fiber Bragg gratings.

Gaixia Xu was born in Inner Mongolia, in 1977. She received the B.Eng. degree in biomedical engineering from the Institute of Changchun Optic Fine Mechanics, Changchun, China, in 2000, and the Ph.D. degree in biomedical engineering from Zhejiang University, Hangzhou, China, in 2005. From 2005 to 2007, she was affiliated with Shenzhen University, Shenzhen, China, as a Postdoctoral Research Fellow. From 2007 to 2008, she was affiliated with the Institute of Laser, Photonics and Biophotonics, State University of New York at Buffalo, Buffalo, NY, USA, as a Visiting Scholar. Since 2008, she has been with Shenzhen University, as an Assistant/Associated /Full Professor. Her current research focuses on biophotonics and nanomedicine.

Yiping Wang (Senior Member, IEEE) was born in Chongqing, China, in 1971. He received the B.Eng. degree in precision instrument engineering from the Xi'an Institute of Technology, Xi'an, China, in 1995, and the M.S. and Ph.D. degrees in optical engineering from Chongqing University, Chongqing, China, in 2000 and 2003, respectively. From 2003 to 2005, he was affiliated with Shanghai Jiao Tong University, Shanghai, China, as a Postdoctoral Fellow. From 2005 to 2007, he was a Postdoctoral Fellow with Hong Kong Polytechnic University, Hong Kong. From 2007 to 2009, he was affiliated with the Institute of Photonic Technology (IPHT), Jena, Germany, as a Humboldt Research Fellow. From 2009 to 2011, he was affiliated with the Optoelectronics Research Centre, University of Southampton, Southampton, U.K., as a Marie Curie Fellow. Since 2012, he has been affiliated with Shenzhen University, Shenzhen, China, as a Distinguished Professor. He has authored or coauthored one book, 21 patent applications, and more than 240 journal and conference papers. His current research interests include optical fiber sensors, fiber gratings, and photonic crystal fibers. Prof. Wang is a Senior Member of the Optical Society of America and Chinese Optical Society.